

Upgrades to the physical modelling lab and upcoming experiments

Marcelo Guarido*, Nasser Kazemi†, Joe Wong*, Nadine Igonin*, Kevin Bertram*, Kristopher Innanen*, and Roman Shor†

ABSTRACT

Physical modelling has been used extensively over the history of CREWES in order to study interesting phenomena and test novel algorithms. In this report, we present updates to the physical modelling laboratory that will allow for more sophisticated experiments and increase efficiency in acquisition. New sources (both P- and S-wave) of various sizes have been purchased, as well as more digitizers that would allow for 24-channel acquisition. Additionally, the source is being upgraded in order to be able to generate complex waveforms that may be more useful for various applications. A seismic while drilling (SWD) experiment is proposed in order to test the capability of SWD signals to enhance subsurface illumination. Using a model with inherent illumination problems, synthetic tests were carried out and used to build up the model to be used in the experiment. Microseismic data geometry is similar to SWD, and the experiment can be repeated, but with a different source pulse for the microseismic events. Preliminary results testing the radiation pattern of various sources are presented, as well as a list of future work that includes elastic physical modelling for SWD, microseismic, and time reversal imaging.

INTRODUCTION

The physical modelling facility has been used for over 30 years for carrying out novel experiments and testing acquisition, processing and imaging algorithms. The lab is a miniaturized version of a real seismic acquisition set-up, with a scale of 1 : 10000. Models are often constructed using material with comparable P- and S-wave velocities to those observed in rocks, such as Plexiglas, which has a P-wave velocity of 2745 m/s, and a density of 1190 kg/m³. So long as the relative properties of the media are such that they produce reasonable reflection and transmission coefficients, the models are a good approximation to reality. P- or S-wave sources can be used, and can be placed anywhere in the model. The only constraint on source position is dictated by the source size, since the frequency is inversely proportional to source size. Additionally, due to the way transducers are built, the S-wave sources are larger than the P-wave sources.

Most often, receivers are on the surface and their position is controlled by a computer system linked with a moving gantry. Multi-channel acquisition is possible, with up to eight receivers being used at once in the past. The use of a computer-guided acquisition allows for the specification of many kinds of geometries, such as regular grids or concentric circles.

In this report, we first describe the upgrades that have taken place or are in the process

*CREWES - University of Calgary

†CFREF - University of Calgary

of being done. Then, we go on to discuss a few new applications of the physical modelling data. Specifically, one of these application is to do with seismic-while-drilling (SWD), which is a technique where seismic data is acquired using the drill bit signal as the source. Another application involves microseismic sources, and time reversal imaging.

UPGRADES TO PHYSICAL MODELLING LABORATORY

The current phase of updates to the physical modelling facility is motivated in part by a collaboration with Dr. Roman Shor in the department of Chemical and Petroleum Engineering at the University of Calgary, through the Canada First Research Excellence Fund (CFREF). The overarching research direction is *Global Research Initiative in Sustainable Low Carbon Unconventional Resources*, of which Theme 2 is *Low Permeability Hydrocarbon Resources*. Within that theme, a more specific research direction is *RT1: Improved Sweetspot Targeting in MFHW's*, wherein the goal is to use drilling data to derive rock mechanical properties in bounding zones and along-well. Seismic-while-drilling (SWD) is directly related to this application, since any methods that aim to improve imaging through SWD would allow for improved sweetspot targeting.

One of the major upgrades has to do with increasing the number of channels for the receivers. The current capacity is for 8 channels, and is run through a *GaGe FCiX Octopus* digitizer (Figure 1). Two more digitizers have been purchased, allowing for 24-channel acquisition. This is expected to increase acquisition speed threefold, which is necessary as the experiments carried out are becoming increasingly complex.

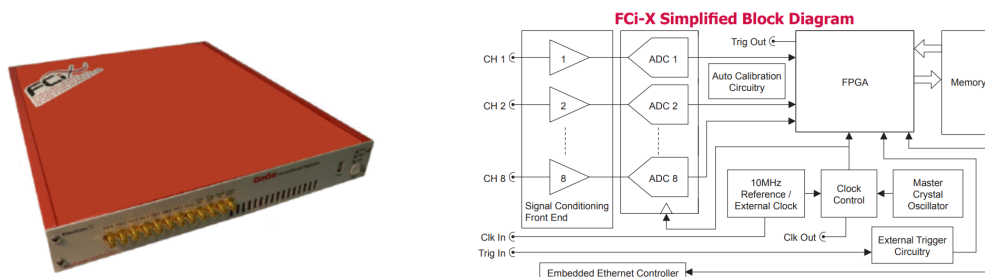


FIG. 1: GaGe FCiX Octopus digitizer (left) and its block diagram (right).

Another important consideration is to do with the size of the sources and receivers. In most applications, it is best to have the source approach the size and behaviour of a point source. Therefore, with the 1 : 10000 scale considered, the smaller the transducers, the better. There are several different kinds of transducers, and one of the thinnest is a piezoelectric pin (Figure 2). The one shown has a diameter of 0.065" (1.62 mm), and there are 36 new ones that have been purchased. These will serve as vertical component receivers in the multi-channel acquisition system, or possibly as sources in some of the experiments described later on.

In addition to the pins, several kinds of S-wave sources have been purchased. For example, Figure 3 shows one such S-wave source that is capable of producing low frequencies (30 Hz in this case). The cost for such low frequency content is the size of the transducer, which for this case is 24 mm in diameter. These transducers can produce and capture horizontal motion. Among many other applications, it is useful for S-wave source surveys, low

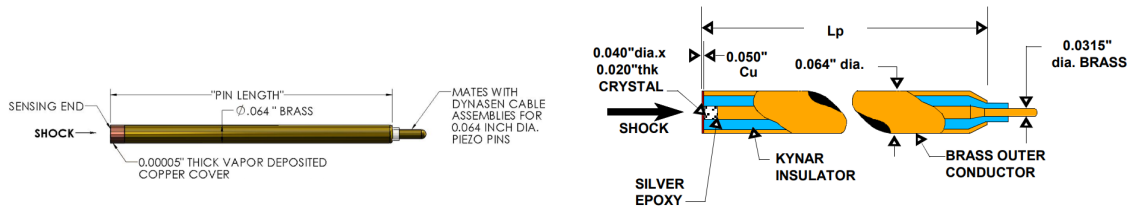


FIG. 2: Components of the piezoelectric pin CA-1135 from Dynasen.

frequency full waveform inversion (FWI) applications, and studying converted waves.

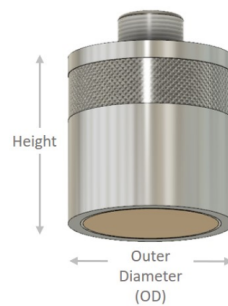


FIG. 3: Circular piezocomposite GS30-D19.

Finally, although the previously described sources will be sufficient for several exciting experiments, they are fundamentally limited in the waveforms they are able to generate. Since a SWD source is inherently complex, a source able to create any waveform given to it would be ideal. Therefore, in the future, methods to do so are going to be explored. The current plan is to purchase and program a Raspberry Pi, as well as a high voltage amplifier in order to enhance the signal to noise ratio.

New model

The motivation for this round of experiments is to test the ability of different algorithms to enhance illumination. To that end, a model with inherent illumination problems is being built (Figure 4). The circles in the bottom layer are embedded high-velocity objects in order to test illumination. Receivers are going to be on the surface, and a baseline seismic survey with sources on the surface can be carried out. Then, a wellbore is going to be drilled into the model and the source is going to be placed inside. The wellbore will be drilled a few millimetres at a time, and the source will be pushed against the bottom at certain increments in depth. The first round of experiments will have v_1 be the velocity of water, and be a purely acoustic experiment. Later iterations will see v_1 replaced with a solid material to allow for elastic sources to be used.

Although this model is simple, in the future, more complex versions of this model are going to be constructed. One possibility being considered is the use of 3D printing to design a complex model that can then be used to redo the same experiments being proposed in the following sections.

In summary, the physical modelling facility is being upgraded with new equipment, and

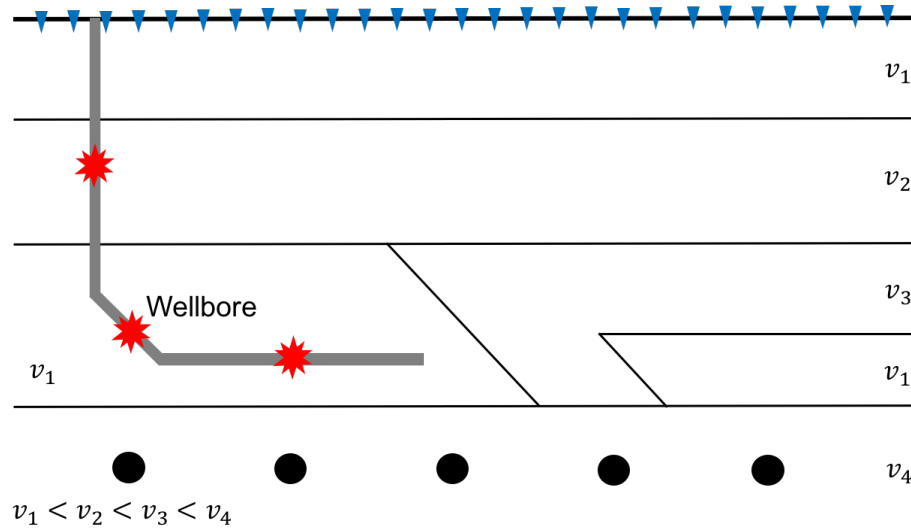


FIG. 4: Cross section of the model in construction, with receivers on the surface and sources to be embedded in the model itself.

new models are being built for experiments. In the following sections, we discuss some of the applications with the upgraded equipment and model being built.

SEISMIC WHILE DRILLING (SWD) EXPERIMENT

Motivations

Surface land and marine seismic data contain reflected waveforms from the subsurface which can be back-propagated through a background medium for imaging purposes. However, in complex structures wave energy can penetrate quite weakly into some areas (i.e. illumination problem). During drilling, a drill-bit generates significant elastic wave energy whose ray paths are unique relative to those induced by standard surface seismic. Moreover, since drilling is necessary, using drill-bit-rock interaction as a seismic source comes with no extra cost or interruption in the drilling process. Hence, provided that we understand the challenges associated with characterizing the source radiation properties of the drill bit- rock interaction, the data arising from seismic-while-drilling (SWD) are complementary to surface data and have the potential to enhance geophysical evaluation of the subsurface. Hence, this brings an opportunity to address the seismic illumination issue by adding new measurements into the imaging problem. In this report, we propose a physical modelling study of the SWD method to mitigate the illumination problem in imaging. Given the differences between drill-bit generated elastic wave energy and that generated by standard sources, we broach this possibility with a physical modelling study. Our intent is to create and validate a workflow that creates clear images of the subsurface which can be used to optimize drilling parameters (Greenberg, 2008).

SWD data and depth imaging

One of the main differences between conventional surface seismic data and SWD data is the source signature. In the case of SWD acquisition, the drill bit-rock interaction generates a correlative and non-impulsive source signature. To mimic the drill bit-rock signature, we

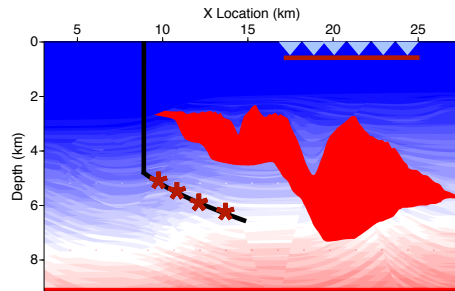


FIG. 5: Seismic-while-drilling acquisition.

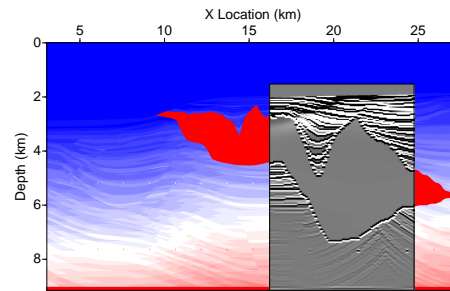


FIG. 6: Imaging result of SWD data over the Sigsbee2a model.

assume that every tooth of the drill bit generates a harmonic waveform (Poletto, 2005). Depending on the velocity of rocks and the drilling parameters, the source signature will have harmonic and non-harmonic components due to the resonances between the drillstring and rocks at the source locations. To make the source signature broadband, we add a band limited white Gaussian noise to the signature. In the next section, we will explain how we can generate such a source in the lab experiment. As our goal is to provide a prestack depth migrated image using the SWD dataset, we need to forward propagate the source side wavefield and then cross-correlate it with the backward propagated receiver side volume. To build the source side wavefield, we need to know the source signature of the SWD dataset.

First, we explore the added value of SWD data on improving the illumination of the subsurface images with a numerical example on the Sigsbee2A model. The numerical examples are borrowed from Kazemi et al. (2018). We start by simulating both surface and SWD data. In the case of SWD data, we use drill bit-rock interaction as sources in the deeper part of the well and put receivers near the surface with 9 km offset from the well's location (Figure 5). In the case of surface seismic, sources are fired near the surface and receivers were listening to all of the shots. To generate the data, we use a second order acoustic finite difference modelling engine and in the case of SWD data, later we convolve the data with a drill bit source signature. To image the SWD data, we estimated the source signature by applying the Sparse Multichannel Blind Deconvolution algorithm (Kazemi and Sacchi, 2014) on one of the shot gathers. A windowed version of the data is depicted in Figure 7a. True drill bit-signature-removed data and the estimated version of it are shown in Figures 7b and c, respectively. Later, we use the estimated drill bit-signature-removed data and drill bit data to estimate the drill bit waveform. The estimated waveform is shown in Figure 7e.

Then, we insert the drill bit signature into the pre-stack reverse time migration algorithm to image the subsurface (Figure 6). It is clear that we are able to successfully image the subsurface. Comparing the SWD image with the surface seismic image, shown in Figure 8a, we notice that under the salt region is nicely imaged by the SWD technique. On the other hand, the surface seismic image suffers from poor illumination. Finally, in Figure 8b, by combining SWD and surface seismic data images, we are able to improve the subsurface image and provide a reliable and clear image of the subsurface that can be used to optimize the drilling parameters and guarantee an efficient rate of penetration. The blue square rectangle in Figure 8b shows the common image region between the SWD and surface

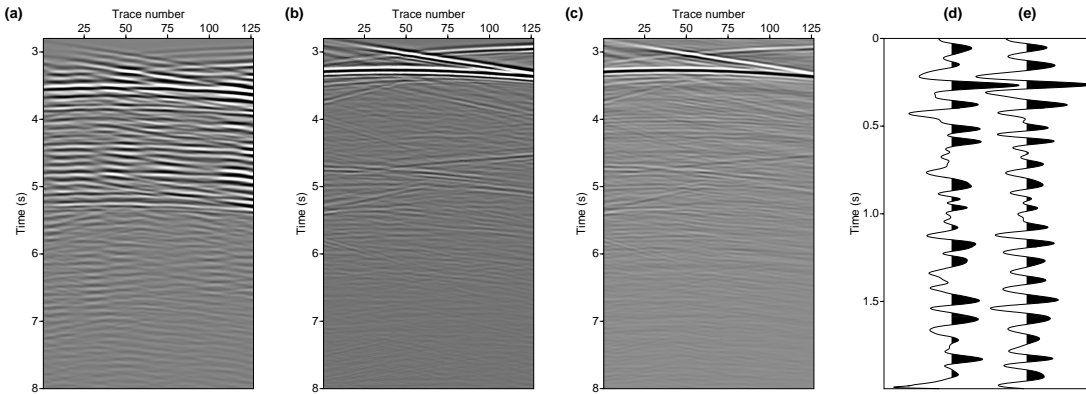


FIG. 7: Windowed version of SWD data. a) SWD shot gather. b) True drill bit source removed data. c) Estimated drill bit source removed data. d) True and e) Estimated source signatures.

seismic images and arrows show the subsalt regions where the combined image did a better job than that of the surface seismic image in improving the illumination. In the combined image, we can easily see the lower boundary of the salt and the point diffractor under it. For more information about the numerical examples, interested readers are referred to Kazemi et al. (2018).

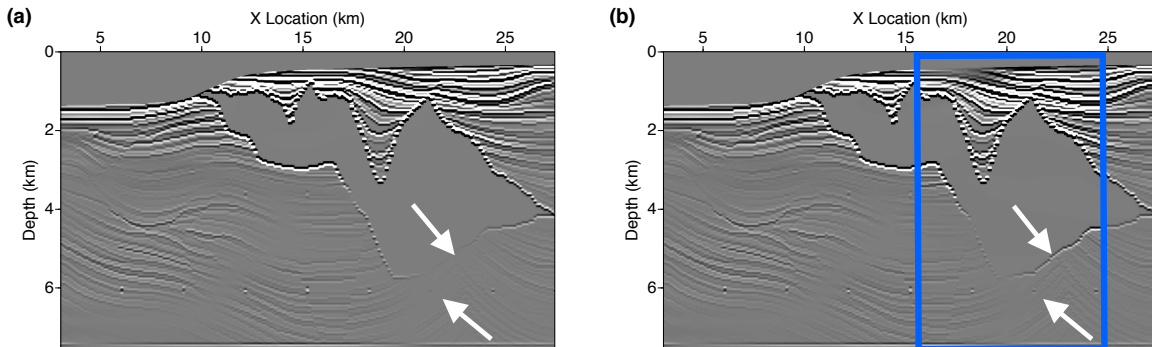


FIG. 8: Prestack RTM images of the Sigsbee2a model. a) Surface seismic imaging. b) Combined SWD and surface seismic imaging.

SWD physical modelling setup

The main goal of this experiment is to acquire a realistic benchmark dataset that simulates SWD acquisition. We will explore the added value of SWD data in improving the illumination of subsurface models and reducing the uncertainties of depth migration. To do so, we designed a simple 2.5 D model with a high-velocity wedge model surrounded by low-velocity layers. The idea is to simulate a subsalt imaging problem and investigate the illumination issues on this model. The schematic representation of the proposed model is shown in Figure 4. In the model, we have $v_1 < v_2 < v_3 < v_4$ where v_1 is the velocity of water and v_3 is the high-velocity wedge layer that resembles a salt body.

SWD acquisition consists of sources in the well location and the receivers at the surface. In conventional surface seismic acquisition rays will bend towards high-velocity barrier region and the layers under the high-velocity wedge layer will be a shadow zone to our

surface seismic. On the other hand, in seismic-while-drilling, rays will propagate from the drill bit-rock interaction and they will illuminate the subsalt region from underneath.

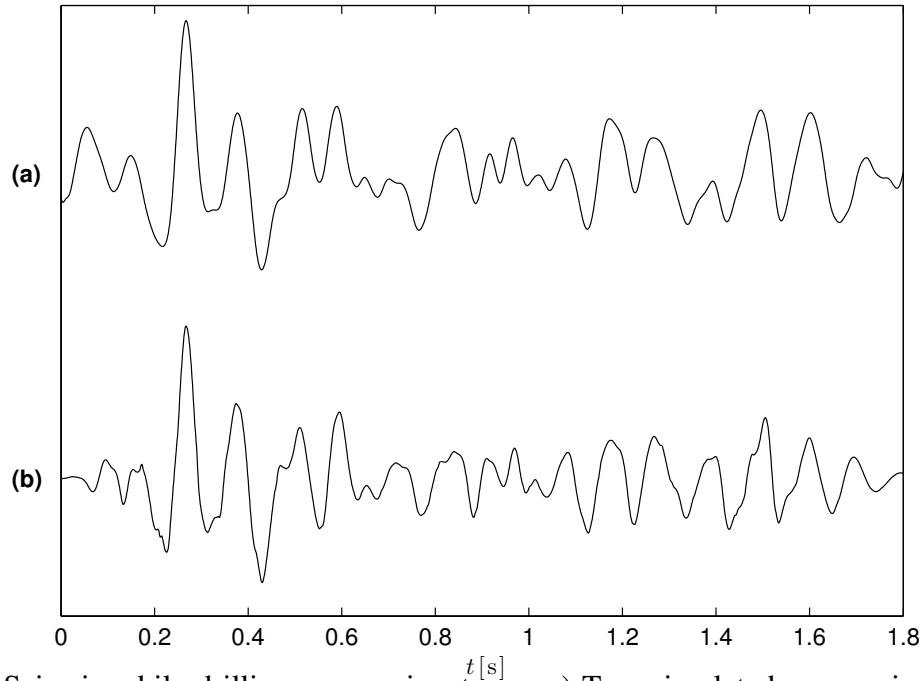


FIG. 9: Seismic-while-drilling source signatures. a) True simulated source signature. b) Approximated source signature that can be generated in the lab.

In the lab, the sources are 12" long CA-1136 piezoelectric pins with standard 0.020" thick PZT-5A crystal discs. These sources can generate damped harmonics with dominant frequencies that are a function of the thickness of discs (see Figures 10a and 10b). On the other hand, the seismic-while-drilling sources have harmonic and non-harmonic components which are dependent on the drilling parameters and the physical properties of the rocks interacting with the drill bit. Accordingly, to simulate the seismic-while-drilling source represented in Figure 9a, we solve for a sparse train that when convolved with the two damped harmonic piezoelectric pin sources, the output approximates the original SWD source signature. In other words, we solve

$$\text{minimize } \|\mathbf{W}_1 \mathbf{W}_2 \mathbf{x} - \mathbf{w}_{SWD}\|_2^2 + \lambda \|\mathbf{x}\|_1, \quad (1)$$

where \mathbf{x} is the sparse train, and \mathbf{W}_1 and \mathbf{W}_2 are convolutional matrices built from the piezoelectric pin sources in Figures 10a and 10b, respectively. Solving equation 1 results in the optimized sparse train shown in Figure 10c. Hence, convolving the two piezoelectric pin wavelets with the sparse train approximates the original SWD source signature. The approximated SWD source signature is represented in Figure 9b. Therefore, with this proposed methodology showing promising results in a synthetic case, we can move forward with acquiring physical modelling data.

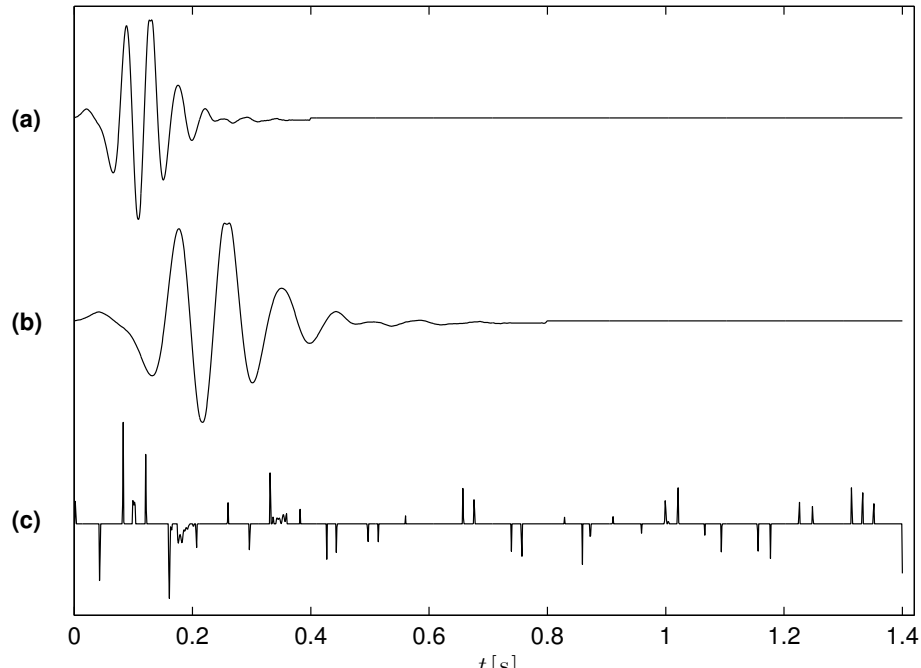


FIG. 10: Approximating SWD source signature $t[s]$ by piezoelectric pin sources and a sparse train. a) Piezoelectric pin with dominant frequency of 25 Hz ; b) piezoelectric pin with dominant frequency of 10 Hz ; c) optimized sparse train after solving equation 1.

MICROSEISMIC EXPERIMENT

The microseismic experiment has very similar motivations to the SWD experiment. Surface seismic surveys can be enhanced by illumination provided by sources in the subsurface. This has been the focus of microseismic full waveform inversion (MFWI), which is a FWI implementation that simultaneously updates the source position (in the subsurface), and the properties of the medium (the velocity model the events propagate through). For the details of the elastic implementation of MFWI, see (Igonin and Innanen, 2018).

The geometry of the SWD experiment is very similar to the geometry of typical hydraulic fracturing stimulations, so the same models proposed in the previous sections can be used for the experiment. However, before any complex experiments can be done, the character of the source needs to be studied carefully. Microseismic sources have a specific focal mechanism associated with them, most often being double couple (strike-slip). Since P- and S-wave transducers are to be used as the source, it is important to know their radiation patterns and how they are similar, or dissimilar, to microseismic sources. One way to test this is by doing a simple transmission experiment, such as the one shown in Figure 11. Using a block of acrylic, a source on the bottom, and an array of receivers on the surface, it is possible to determine the radiation pattern.

To begin with, a P-wave transducer was used as the source on the bottom, and piezoelectric pins were used as receivers on top. Therefore, it is a P-P survey, with only the vertical component being recorded. An example shot gather is shown in Figure 12, with each trace normalized by its maximum. P- and S-wave arrivals have been highlighted, but there are also several other complex arrivals that can be seen. These are likely to be a com-

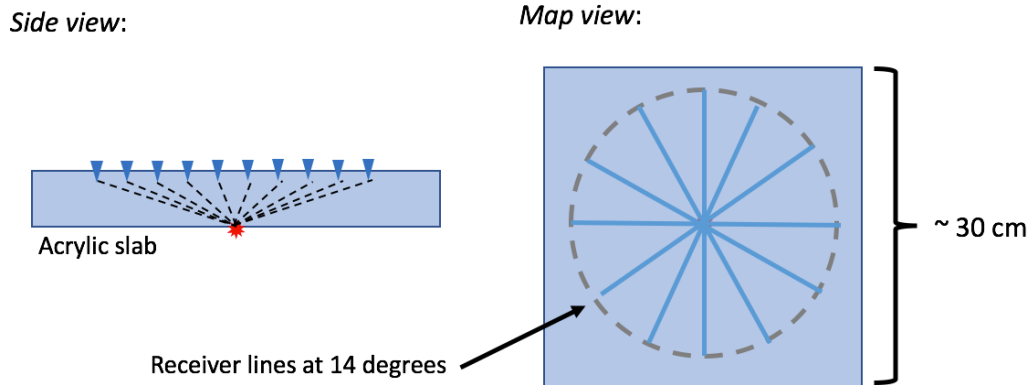


FIG. 11: Schematic of the transmission experiment to study source radiation patterns.

combination of reflections, internal multiples, refractions, and conversions. Therefore, even though this is only a transmission experiment through one layer, the recorded data already shows complexity. It is expected that the full model proposed in Figure 4 will have similar complexities.

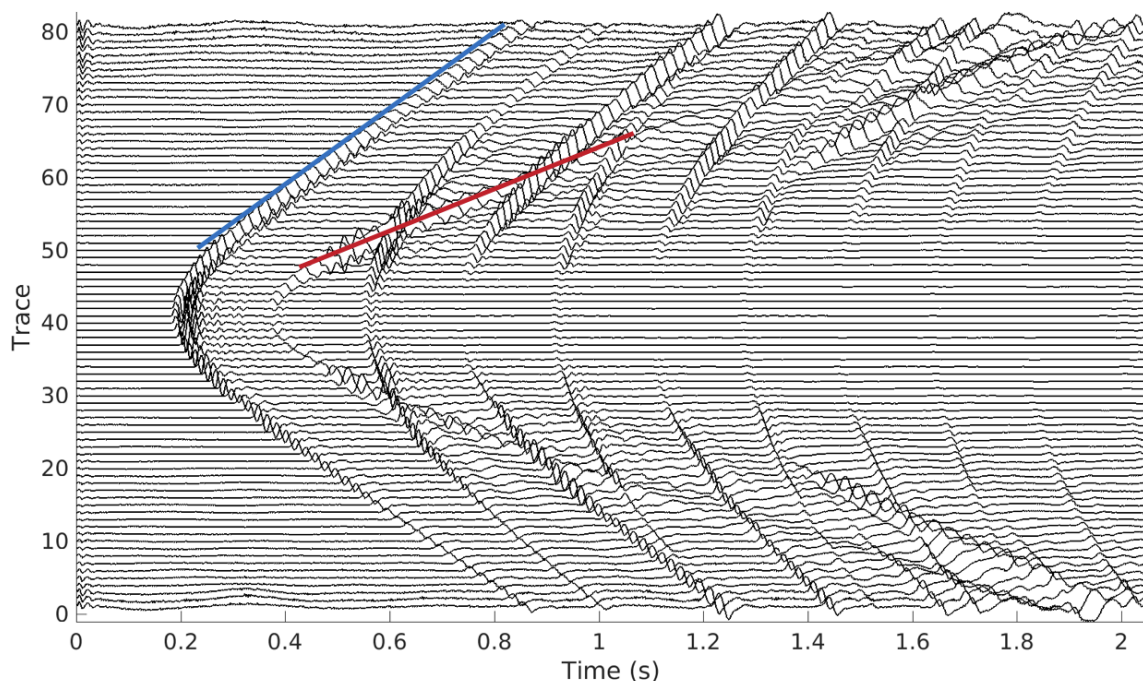


FIG. 12: Example raw shot gather for the 90° azimuth line, with P-wave highlighted in blue, and S-wave highlighted in red.

Polarities are important for the microseismic problem, since a double couple source will have both P- and S-wave polarity reversals. However, as we can see in Figure 13, the P-wave polarity remains positive across the shot gather. The S-wave polarity is mostly positive, with some negative polarity near the zero offset.

To get a better understanding of the behaviour of the amplitudes across the survey, the P-wave arrival time and amplitude were picked at every receiver, and the corresponding maps are shown in Figure 14. Overall, the P-wave transducer appears to be best described

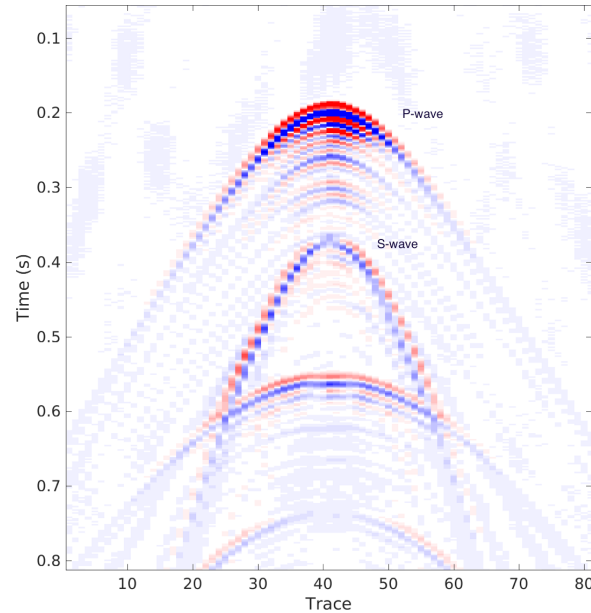


FIG. 13: Example raw shot gather for the 90° azimuth line plotted in terms of amplitude, with red colours signifying positive amplitudes, and blue colours signifying negative amplitudes.

as an explosive source, with positive P-wave polarities across the recording area. The only anomaly is the "x" type pattern with larger arrival times and lower amplitudes at 45° lines. Due to the gradual change in amplitudes seen in Figure 14b, the anomalous behaviour at the 45° lines is likely due to the directivity of the source, but future work will explore this further.

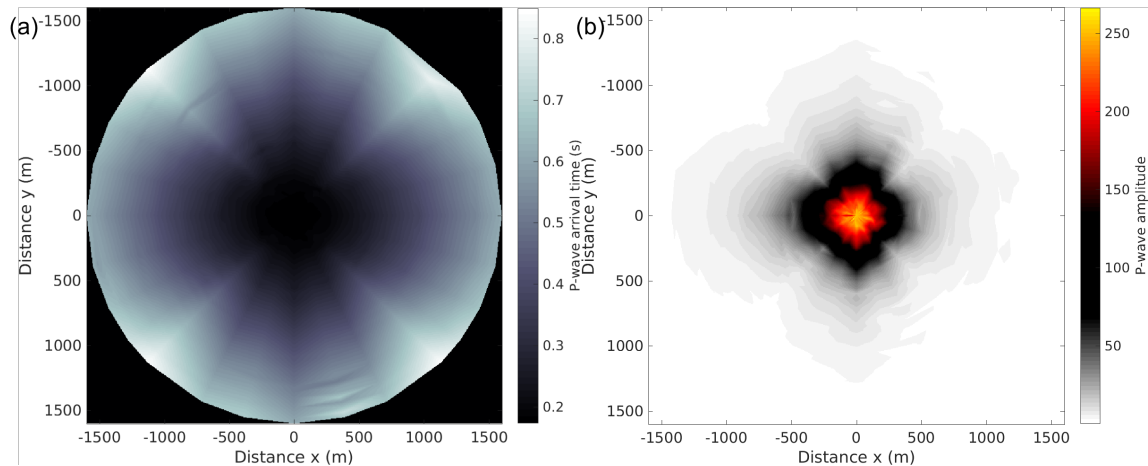


FIG. 14: P-wave arrival time and amplitude for the transmission experiment. a) Arrival time; b) amplitude. The distance is in meters scaled with a ratio of 1:10000, and the amplitudes are obtained from the raw data without any instrument response corrections.

FUTURE WORK

This report serves mostly as a proposal of work to be done, so various elements of future work have already been discussed previously. Namely, adding complexity to the source, and the model being used, are two directions of future work. Another focus of future

work is to test the application of time reversal (TR) imaging. This method can be simply illustrated in Figure 15. Initially, a source goes off somewhere in a complex, heterogeneous medium, and is recorded by receivers at some distance away. Then, the receivers are turned into sources and they send the signal back into the medium that they recorded. Due to wavefield reciprocity, the wavefronts end up converging at the source location.

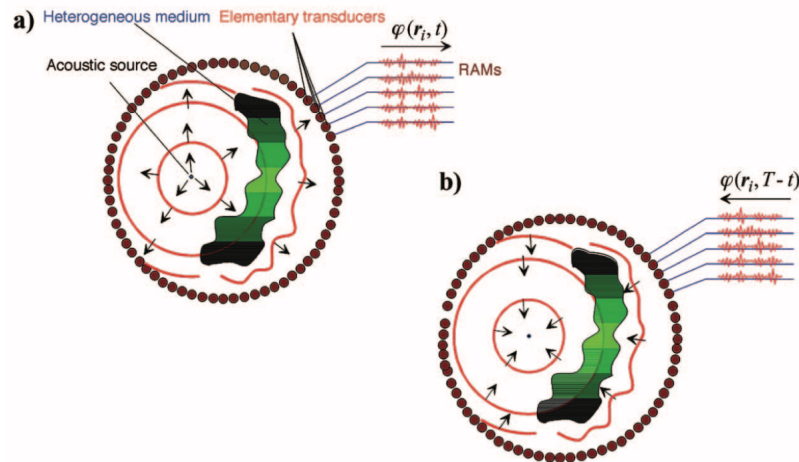


FIG. 15: Concept of time reversal imaging from Fink (2006). (a) Emission from original source and recording at receivers. (b) Sending recording back into medium from position of receivers.

In practice, this method has been most widely applied to physical laboratory data, due to the inherent ability of the receivers to become sources. It has also been used for medical imaging, and for locating caverns (Fink, 2006). Aside from the pure academic interest, and interesting parallel with time mirrors (Innanen, 2018), further thought is required to determine practical applications of this method for seismic data.

CONCLUSIONS

Promising new experiments involving seismic while drilling, microseismic and time reversal imaging are planned for the upgraded physical modelling facility. Preliminary results using synthetic data for SWD are presented, as well as some initial study into the character of the sources that can be used in the microseismic experiment. Future work involves further upgrades to the equipment, the addition of the ability to generate complex waveforms, and the creation of increasingly complex models.

ACKNOWLEDGEMENTS

The authors thank the sponsors of CREWES for continued support. This work was funded by CREWES industrial sponsors and Natural Science and Engineering Research Council of Canada (NSERC) through the grant CRDPJ 461179-13. This work was also funded through the Canada First Research Excellence Fund (CFREF).

REFERENCES

Fink, M., 2006, Time-reversal acoustic in complex environments: *Geophysics*, **71**, No. 4, P.S1151–S1164.

- Greenberg, J., 2008, Seismic while drilling keeps bit turning to right while acquiring key real-time data: *Drilling Contractor*, **64**, No. 2, 44–45.
- Igonin, N., and Innanen, K., 2018, Elastic microseismic full waveform inversion: synthetic and real data: *CREWES Research Report*, **30**.
- Innanen, K., 2018, Space-time boundary reflections in elastic media: *CREWES Research Report*, **30**.
- Kazemi, N., and Sacchi, M. D., 2014, Sparse multichannel blind deconvolution: *Geophysics*, **79**, No. 5, V143–V152.
- Kazemi, N., Shor, R., and Innanen, K., 2018, Illumination compensation with seismic-while-drilling plus surface seismic imaging, *in* 80th EAGE Conference and Exhibition 2018.
- Poletto, F., 2005, Energy balance of a drill-bit seismic source, part 1: Rotary energy and radiation properties: *Geophysics*, **70**, No. 2, T13–T28.